



Original Research

The Cochlear Size Variations in Incomplete Partitions with Multiplanar Images on Pediatric Temporal Bone CT

Direnc Ozlem Aksoy,¹ Emine Meltem,¹ Yesim Karagoz,¹ Melis Baykara Ulsan,¹
 Ozdes Mahmutoglu,² Abdullah Soydan Mahmutoglu¹

¹Department of Radiology, University of Health Sciences Türkiye, Istanbul Training and Research Hospital, Istanbul, Türkiye

²Department of Radiology, University of Health Sciences Türkiye, Sisli Hamidiye Etfal Training and Research Hospital, Istanbul, Türkiye

ABSTRACT

Objectives: The purpose of the study was to evaluate cochlea dimensions by the multiplanar reconstruction of high-resolution computed tomography that could be useful in diagnosing incomplete partition (IP) malformations.

Methods: This study included 32 patients with 64 side cochleae diagnosed with IP defect and 38 cochleae as the control without any defect. Basal turn length (BL), cochlear height (CH), Mid-apical length (MAL), Mid-apical height, Cochlear length (A), and Cochlear width (B) were measured on reformat images.

Results: Twenty cochleae of these patients have been diagnosed with IP type I, 34 with IP type II, and 10 with IP type III. The MAL values are shorter than the control group in IP types I and III ($p<0.001$, $p<0.001$). BL values are shorter in IP type III cases ($p<0.001$). In IP II cases, BL and MAL values overlapped with the control group. CH did not differ significantly from the control group in any IP type. A and B values were significantly lower than the control group for IP I and III ($p<0.01$). There is a positive correlation between A and B values for all IP types ($p<0.01$).

Conclusion: Quantitative data about differences in the size and shape of the cochlea in IP cases would help differentiate them from the normal cochlea. Since A and B values showed a positive correlation, it is suggested that A and B values can be used to estimate CDL for IP types.

Keywords: Cochlea, cochlear measurements, incomplete partition, temporal CT

Please cite this article as "Aksoy DO, Meltem E, Karagoz Y, Baykara Ulsan M, Mahmutoglu O, Mahmutoglu AS. The Cochlear Size Variations in Incomplete Partitions with Multiplanar Images on Pediatric Temporal Bone CT. Med Bull Sisli Etfal Hosp 2023;57(3):426–433".

Inner ear anomalies constitute 20% of congenital sensorineural hearing loss (SNHL) cases. Imaging the temporal bone with computed tomography (CT) and magnetic resonance imaging is essential in revealing these anomalies. Diagnosis of inner ear anomalies is important in planning treatment. The current diagnosis and classification of inner ear anomalies are based on the visual evaluation of temporal bone CT.^[1] Although it is not difficult to recognize severe

inner ear anomalies (complete labyrinthine aplasia, cochlear aplasia, etc.) by visual evaluation of images, it can be challenging to identify milder cochlear abnormalities (cochlear hypoplasia, incomplete partitions [IP], etc.).^[2] Standardized quantitative data that can be used in the diagnosis can be helpful in the classification of inner ear abnormalities to reduce the importance of the radiologist's experience performing the evaluation and technical limitations.

Address for correspondence: Direnc Ozlem Aksoy, MD. Department of Radiology, University of Health Sciences Türkiye, Istanbul Training and Research Hospital, Istanbul, Türkiye

Phone: +90 505 398 63 38 **E-mail:** direncozlemaksoy@gmail.com

Submitted Date: April 04, 2023 **Revised Date:** June 06, 2023 **Accepted Date:** August 04, 2023 **Available Online Date:** September 29, 2023

©Copyright 2023 by The Medical Bulletin of Sisli Etfal Hospital - Available online at www.sislietfaltip.org

OPEN ACCESS This is an open access article under the CC BY-NC license (<http://creativecommons.org/licenses/by-nc/4.0/>).



Cases with modiolar hypoplasia and interscalar septal defects in the cochlea were classified as IP defects. According to the classification made by Sennaroğlu and Bajin, IP cases constitute approximately 40% of inner ear anomalies. IP cases are divided into three types according to the degree of modiolar hypoplasia. While IP type I gives a cystic cavity appearance of the cochlea due to modiolar and interscalar septal defects, IP type II has the cystic cavity appearance only at mid-apical turn due to partial defects of these structures. IP type III (X-linked deafness) shows the cochlea's typical "corkscrew" appearance due to an intact scalar septum with the complete absence of modiulus.^[1]

The evaluation of the inner ear structures with the temporal bone CT is the first choice because of its high resolution for assessing the bony labyrinth. However, the diagnostic accuracy of radiology in daily practice can be increased if standardized quantitative measurements are used rather than qualitative visual evaluation. Some studies in the literature have tried to reveal normal measurements of inner ear structures in SNHL cases.^[3-7] However, since inner ear anomalies have very different bony labyrinth configurations, evaluating them all under the same heading would not be correct. Studies conducted on SNHL cases either did not include cochlear anomalies or did not have enough numbers to evaluate anomalies separately.^[4,8,9]

Although several studies have been conducted to evaluate the dimensions of cochlear hypoplasia, we did not find a similar study for IP cases.^[10] Specific measurements for cochlea with IP types should be assessed with the number of cases sufficient for statistical evaluation.^[11]

To standardize the measurements, we only studied the cases with IP defects in our study. We aimed to establish normative measurements of the cochlea in IP cases to facilitate the diagnosis of IP malformations. Due to the lack of reference values to cover all IP types in the literature, we tried to obtain quantitative data and compare them with normal cochlea measurements.

Methods

This study was conducted with the approval taken from the Institutional Clinical Research Ethics Committee in accordance with the principles of the Declaration of Helsinki Ethics committee (Date: November 11, 2022 Decision No: 352).

Subjects

We retrospectively reviewed the picture archiving and communication systems (PACS) system for high-resolution temporal CT of patients diagnosed with IP defects from January 2017 to January 2022. High-resolution temporal

CT is routinely obtained independently of the study in the management of the diagnosis and treatment processes of these cases with SNHL. The diagnosis of patients with IP malformation is based on the classification of Sennaroğlu and Bajin in our radiology department.^[1] When we eliminated the images with artifacts that were not suitable for measurement, we had 32 patients with 64 side cochleae diagnosed with IP. PACS was reviewed for temporal CT scans on similar dates to create a control group for comparison. 38 cases whose cochlea were reported as normal, with no complaints of hearing loss, and who underwent CT images because of otitis media, ear trauma (without fracture), tinnitus, and vertigo were randomly and consecutively enrolled for the control group. The exclusion criteria of this study for the patient and the control group were a previous skull base or temporal surgery history, facial or skull base trauma with fracture, and calvaria deformities.

Imaging

All CT studies were performed at our institution using a standard temporal bone protocol with a 64-slice CT (MSCT; Brilliance 64, Philips Medical System, Best, the Netherlands).

The scans were obtained as a routine HRCT of temporal bone imaging in the supine position with the scanning baseline parallel to the orbitomeatal line. The scanning parameters were kVp=120, mAs=100, FOV=240 mm, and slice thickness=0.5 mm.

Image Reconstruction

The axial images were uploaded to the dedicated software tool on the workstation of IntelliSpace Portal, V5.0.2.40009 (Philips Healthcare), for multiplanar reconstruction (MPR). The raw data were reconstructed into coronal, axial, and sagittal images using bone kernel and considering the anatomical structure of the cochlea. Reformat images were planned according to the macrostructure of the cochlea to eliminate the illusions that may arise from the positional changes of the cases during scanning. It is important to measure from the described standard plan to prevent application differences. Since the axial plan is accepted as a standard for evaluating cochlea, and the measurements obtained from the axial plan can be repeated more easily in the daily routines, we used axial images for cochlea dimensions measurements. Axial and sagittal images were reconstructed perpendicular to each other. Both passed through the cochlear nerve canal midpoint and the apical point of the cochlea. We identified the axial reference image as a plane including the midportion of the modiulus, the round window, and the farthest point of the basal turn. The standardized cochlear image, defined by Escudé et al.,^[12] Xu et al.,^[13] and Schurzig et al.,^[14] was created parallel to the basal

turn on the axial and the sagittal images. Although generating standardized cochlear images with MPR takes extra time, it is a useful way to standardize the measurements. This reformatted image was created on the plane where the oval and round window is visible, and the basal rotation is observed in the broadest way. A and B measurements were made in this plan. We reconstituted the reference axial im-

age using the standardized cochlear image to obtain the plane with the most extended basal turn length (BL), passing through the round window. This axial reference image was created for each cochlea, and all measurements except A and B were made in this plane. A single author (EM) made the measurements of all cases. Reformat images were also created by the same author (Figs. 1-5).

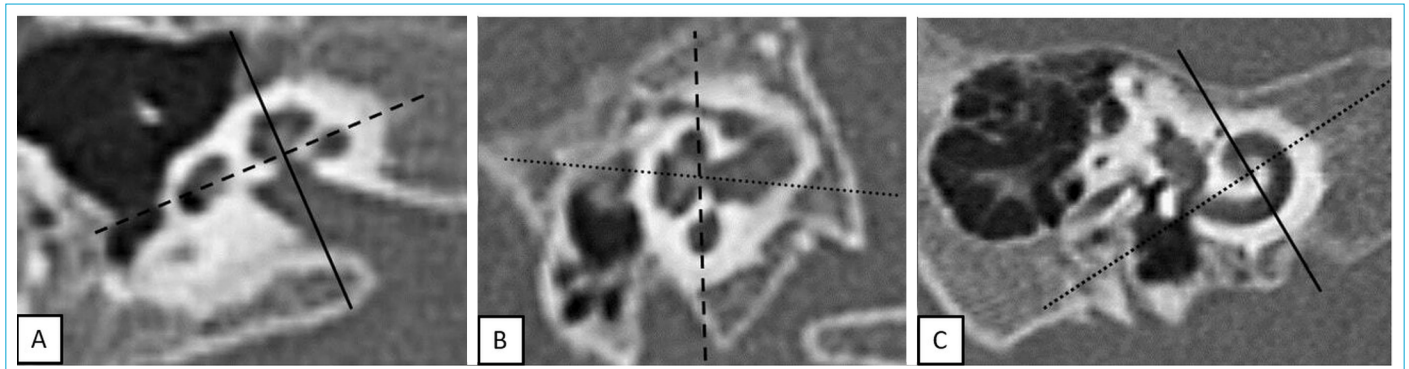


Figure 1. (a) Axial, (b) sagittal, and (c) standardized cochlear images on MPR images. The straight line passes perpendicular to the cochlear nerve canal and the dashed line is parallel to the basal turn in (a) and (b). The dotted line through the midportion of the modiolus to the farthest point of the basal turn in (c).

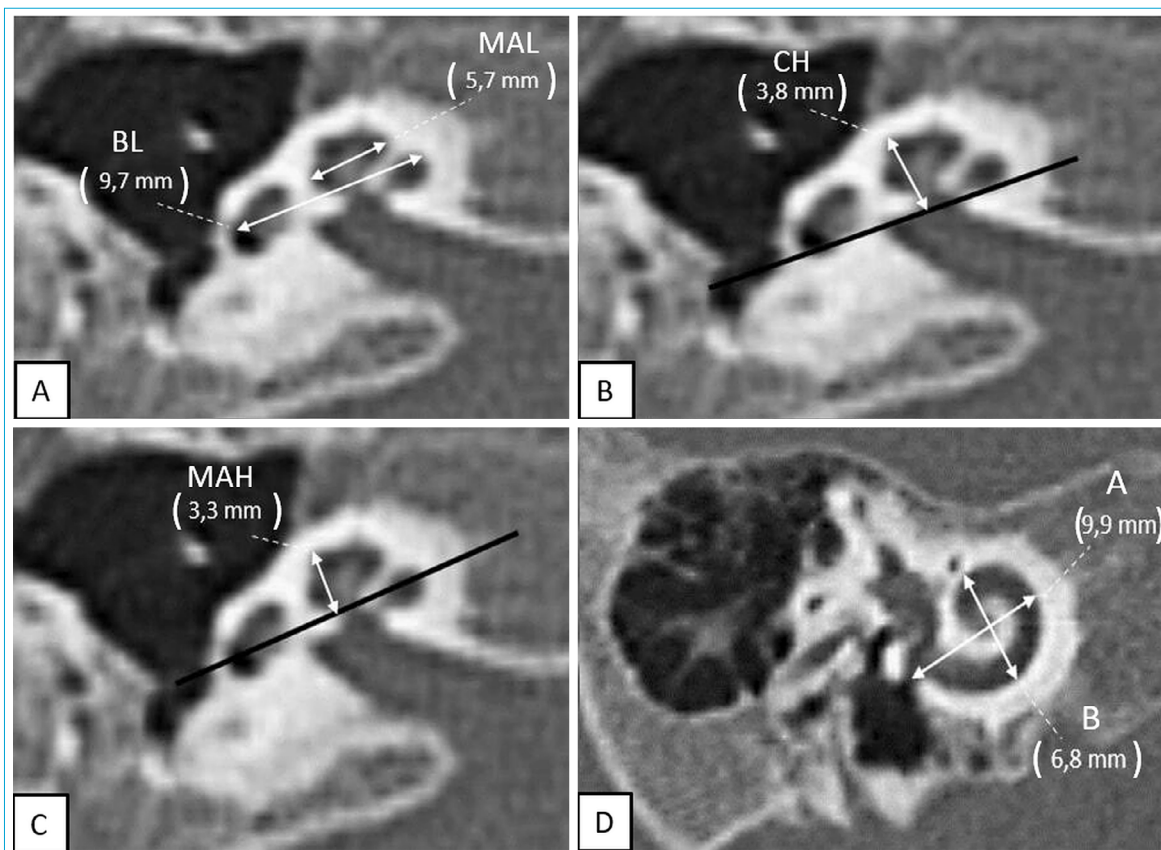


Figure 2. (a-c) Axial inner ear measurements of a normal cochlea. (a) MAL and BL (b) CH (black line passing parallel to the basal turn). (c) MAH (black line passing parallel to the middle apical turn). (d) A and B on the standardized cochlear image (CH: Cochlear height; BL: Basal length; MAH: Mid-apical height; MAL: Mid-apical length; A: Cochlear length; B: Cochlear width).

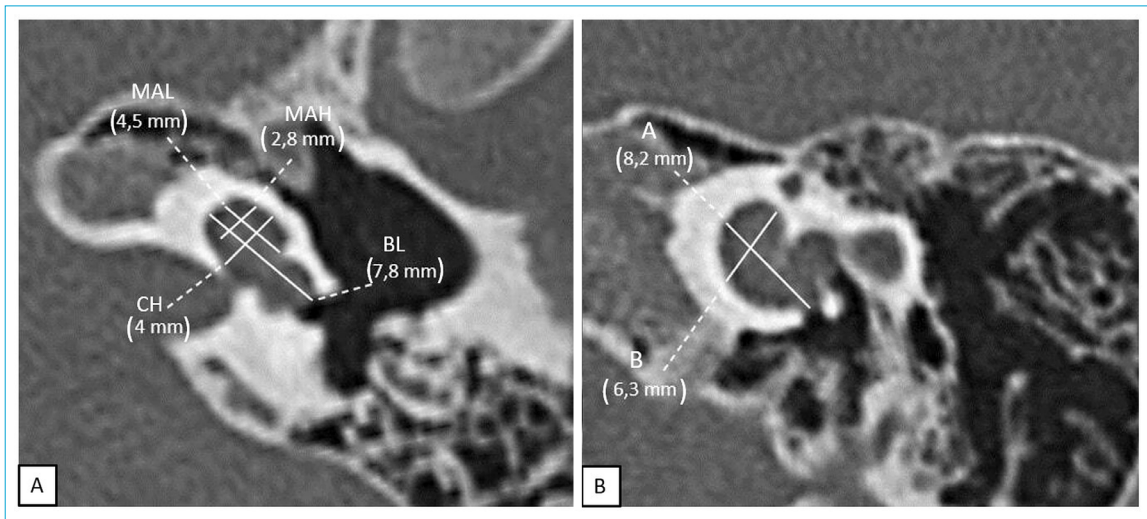


Figure 3. (a) Axial and (b) standardized cochlear measurements of the inner ear in IP I patient. (CH: Cochlear height; BL: Basal length; MAH: Mid-apical height; MAL: Mid-apical length; A: Cochlear length; B: Cochlear width).

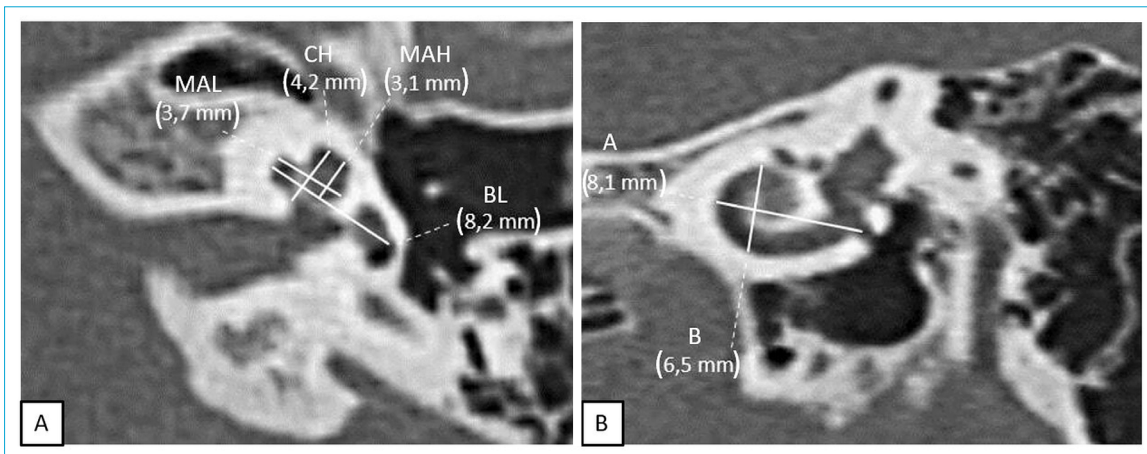


Figure 4. (a) Axial and (b) standardized cochlear measurements of the inner ear in IP II patient. (CH: Cochlear height; BL: Basal length; MAH: Mid-apical height; MAL: Mid-apical length; A: Cochlear length; B: Cochlear width).

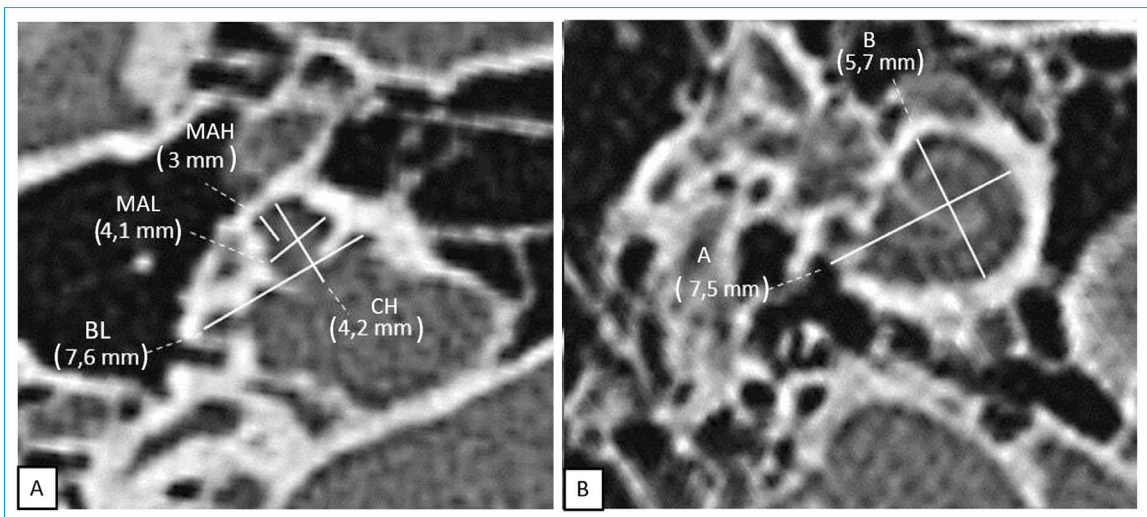


Figure 5. (a) Axial and (b) standardized cochlear measurements of the inner ear in IP III patient. (CH: Cochlear height; BL: Basal length; MAH: Mid-apical height; MAL: Mid-apical length; A: Cochlear length; B: Cochlear width).

Measurements

Measurements on axial images

- BL: A line extending from the midpoint of the round window to the distal point of the cochlear basal turn.^[11]
- Cochlear height (CH): A perpendicular line from the cochlear basal turn to the apical point of the cochlea.^[11]
- Mid-apical length (MAL): A line between the endpoints of the mid-turn of the cochlea on the axial reference image.^[3]
- Mid-apical height (MAH): A line from the apical point down to the line separating basal and upper turns (base of modiolus to apical end).^[3]

Measurements on standardized cochlear image:

- Cochlear length (A): A straight line running from the round window through the center of the cochlea to the farthest point on the opposite wall of the cochlea.^[12,14]
- Cochlear width (B): A straight line running between the two opposite side walls of the cochlea, perpendicular to the A, passing through the center.^[12,14]

Statistical Analysis

Mean, standard deviation, median, minimum, maximum value frequency, and percentage were used for descriptive statistics. The distribution of variables was checked with the Kolmogorov–Smirnov test. Independent samples t-test and Mann–Whitney u-test were used to compare quantitative data. The correlation between variables was tested with Spearman Correlation. IBM SPSS Statistics for Windows, version 28.0 (IBM Corp., Armonk, N.Y., USA) was used for statistical analyses.

Results

This study included 32 patients (18 males and 14 females) with 64 side cochleae diagnosed with IP. Twenty cochleae of these patients have been diagnosed with IP type I, 34

with IP type II, and 10 with IP type III. 8 patients had bilateral IP type I (remaining 4 malformed cochleae was from patients with unilateral IPI), 16 had bilateral IP type II (remaining 2 IPII cases were unilateral), and 5 had bilateral IP type III malformed cochlea. There were 19 (38 sides) control cases, with 26 females and 12 males. The mean age of the IP type I group was 54.7±59.7 months, the IP type II group was 68.5±55.8 months, the IP type III group was 140.4±70.0 months, and the control group was 70.2±52.1 months.

Descriptive data from the measurements of each IP type and control group are presented in Table 1. While BL values in IP type I cases did not differ significantly from the control group, they were shorter in IP type III cases ($p<0.001$). The MAL values are shorter than the control group in IP types I and III ($p<0.001$, $p<0.001$). BL and MAL values in IP type II cases overlapped with the control group. CH did not differ significantly from the control group in any IP type ($p>0.05$).

The mean values of A were IP I 8.5±0.6 mm, IP II 8.9±0.4 mm, and IP III 8.2±0.4 mm. The mean values of B were IP I 5.9±0.5 mm, IP II 6.6±0.6 mm, and IP III 5.3±0.6 mm. A and B values were lower than the control group for all IP types. However, this difference is statistically significant in IP type I ($p=0.06$, $p<0.01$) and IP type III ($p<0.01$, $p<0.01$) cases but insignificant in IP type II cases ($p=0.700$, $p<0.148$). There is a positive correlation between A and B values for all IP types ($p<0.01$) (Table 2 and Fig. 6).

Table 2. Spearman correlation between A and B in control and all IP groups

	Control	IP I	IP II	IP III
	B (mm)	B (mm)	B (mm)	B (mm)
A (mm)				
r	0.291	0.466	0.394	0.531
p	0.076	0.000	0.001	0.000

IP: Incomplete partition; A $p=0.05$ or lower was considered statistically significant.

Table 1. The comparison of inner ear measurements of each IP type with the control group

	Control	IP I		IP II		IP III	
	Mean±SD	Mean±SD	p	Mean±SD	p	Mean±SD	p
BL	9.2±0.4	8.9±0.7	0.153	9.2±0.4	0.747	8.1±0.5	0.000
MAL	5.2±0.4	4.6±0.8	0.01	5.3±0.5	0.700	3.6±0.6	0.000
MAH	3.2±0.4	3.2±0.6	0.857	3.5±0.7	0.020	2.9±1.1	0.161
CH	4.0±0.3	4.1±0.7	0.250	3.9±0.4	0.798	3.7±0.6	0.267
A	9.07±0.4	8.56±0.6	0.006	8.20±0.48	0.700	8.28±0.48	0.000
B	6.87±0.3	5.99±0.5	0.000	5.25±0.69	0.148	5.39±0.69	0.000

IP: Incomplete partition; BL: Basal turn length; MAL: Mid-apical length; MAH: Mid-apical height; CH: Cochlear height; A: Cochlear length; B: Cochlear width; A $p=0.05$ or lower was considered statistically significant.

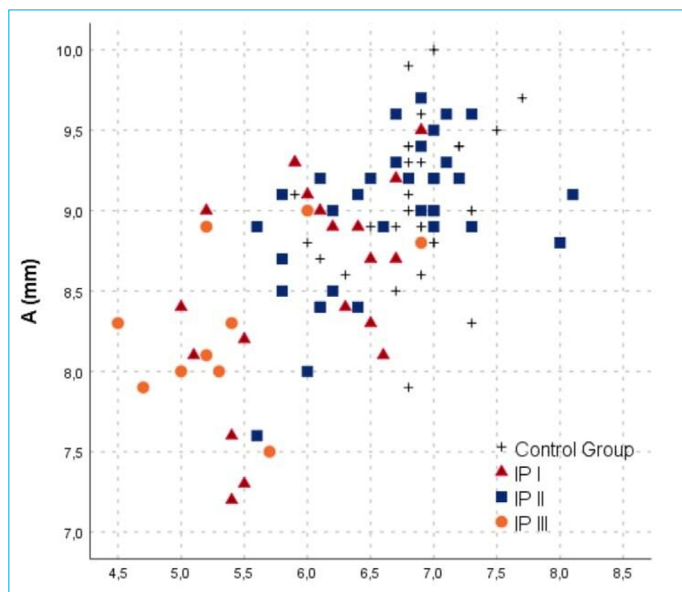


Figure 6. Spearman Correlation of A and B values in the control group and IP cases.

Discussion

Cochlear measurement methods needed to be more consistent with one another. Purcell et al.^[3] made the measurements on coronal and axial views, and the measurements were affected by the position of the head during the scanning. Many following studies used MPR to ensure that the results of the measurements were consistent and reflected the actual size of the cochlea. We measured the cochlea dimensions by MPR to ensure the reproducibility of measurements to reveal the normal value ranges for the quantitative diagnosis of IP malformation. Sennaroglu et al.,^[15] made their measurements as suggested by Purcell et al.^[3] on axial images. In their study that is evaluating IP type I (13) and IP type II (18) cases, they found no significant difference between IP types and normal cochlea for CH and length of the basal turn, whereas Teissier et al.,^[16] made standardized measurements on axial images, using MPR. They compared SNHL cases with control group; however, only Mondini malformation was evaluated separately among cochlear malformations. In this study, CW values (corresponding our MAL measurement) were lower in Mondini cases (5.46 ± 0.62 mm) than in control cases (5.75 ± 0.31 mm).^[16] In our study, we did not detect any significant difference in the dimensions of IP type II cases, except for MAH compared to control cases.

They showed that the width of the second turn of cochlea (CW) values of the Mondini malformation cases was higher than the control group, and the height of the cochlea (CH) values was lower than the control group. However, they did not make a statistically separate evaluation for this group.

Liu et al.^[11] measured CH by MPR in a population with 2 IP type I and 61 IP type II. Since there were few IP type I cases, they could not make statistical analysis. In their evaluation, they found the CH of IP type II cases (3.79 ± 0.13 mm) to be higher than the normal group (3.59 ± 0.12), although they partially overlapped ($p < 0.05$). Dhanasingh^[17] included all three IP types (8 IP type I, 3 IP type II, and 4 IP type III), although their numbers were small. The CH values of IP types and control cases were similar ranging between 4 and 5 mm. In our study, the dimensions of CH of all three groups and the control group largely overlapped (Table 1). Besides this, MAH values were higher in IP type II cases when compared to the control group; no significant difference was found in IP type I and IP type III cases ($p > 0.05$, $p > 0.05$). This reveals that the mid-upper turn height may have increased secondary to the cystic apical union in IP type II cases.

Even though, BL was shorter in IP type III cases than the control group ($p < 0.05$), we found no significant difference in BL values of IP I and IP II cases when compared with the control group. Like the basal turn, we found that the MAL was narrow in IP type III cases. This shows us that the cochlear width of the IP type III cases is narrow, although the total and mid-upper turn heights do not differ significantly compared to the normal cochlea. In a study which cochlear configurations were evaluated with 3D modeling in IP type III cases, the cochlea was defined as narrow after basal turn, which supports our study.^[17]

Escudé et al.^[12] reported that A and B had a linear correlation. The mean A value was 9.23 mm (SD 0.53) and B was 6.99 mm (SD 0.37) in Escudé et al.'s study. Therefore, they used a constant derived from the ratio A/B, assuming A/B as 1.32 in the formulation they defined for the CDL estimation. However, in their study of the temporal bone, CT was randomly selected from patients with the reported otological disease. Meng et al.^[18] defined that the ratio of A and B is inconsistent and can vary significantly from one cochlea to another in normal cases without cochlear anomalies. In his study, Dhanasingh^[17] found A values between 7 and 9.6 mm for IP types I, II, and III. However, this study could not make a statistical comparison due to the small sample size (IP type I 8, IP type II 3, and IP type III 4). The A values of the normal cochleae in Khurayzi et al.'s^[19] study compared to the cochleae with IP type I ($p = 0.049$), IP type II ($p = 0.038$), and IP type III ($p < 0.001$) were significantly different. Some authors argued that the A-value could only be applied to inner ears with normal anatomy.^[17-19] In Liu et al.'s^[11] study, the normal value of CL (A) was 8.84 ± 0.29 mm, and the CW (B) was 6.30 ± 0.38 mm. When they evaluated the IP-II group, the mean A (8.67 ± 0.27 mm) value was slightly smaller ($p < 0.05$) than the normal group but partially overlapped. Besides, CL and CW, in the normal and malformation group,

showed a linear correlation ($p < 0.01$). Therefore, they argued that both could reflect the size of the cochlear basal turn in normal and malformed ears and easily estimate CDL. Therefore, they speculated that the formula proposed by Escudé et al. for CDL calculation was also applicable to the malformed cochlea, combined with literature reports.^[11,20,21] In our study, the mean A value was 9.0 ± 0.4 mm, and the B value was 6.8 ± 0.3 mm in the control group. We did not show any correlation between A and B in control. A and B values were lower than the control group for all IP types. There was considerable overlap between the A and B values of the IP type II and the control group, and no significant difference was found to distinguish them from each other. However, this difference from the control group was statistically significant in IP type I and IP type III cases. Besides this, we found a positive correlation between A and B values for all IP types. This result gives the impression that A and B values can be used in estimating the cochlear canal length, despite the deterioration in their anatomical configuration. Our study supports the few other studies in the literature which speculated that the estimation of CDL was also applicable to the malformed cochlea.^[20-23]

There are some limitations because of the retrospective nature of this study. The main limitation of our study is that a single researcher made the measurements, and intra- and inter-observer correlation assessments were not performed. However, a strict measurement protocol was established to ensure the standardization of measurements and to reduce intra-observer variability. Especially since the incidence of IP type III malformations is low in the population, increasing the number of cases has not been possible. This limitation can only be overcome by increasing the number of cases with the joint participation of different centers. Since other cochlear malformations were not included in the study, data that could be useful in differentiating malformations could not be evaluated.

Conclusion

Differences in the size and shape of the cochlea in various malformations necessitate the establishment of anatomical standards for each malformation group. In this study, we revealed the cochlea dimensions of each type of IP separately. BL and MAL of IP type III cases are shorter and narrower than normal cases. In IP type II cases, the mid-upper return height increased, which may be secondary to the cystic apical union. MAL is short in IP type I cases like IP type II cases. A and B values were lower than the control group in all IP types. However, this difference is statistically significant in IP type I and III but insignificant in IP type II. These quantitative data can help diagnose the IP types by showing the differences from the normal cochlea. Besides this, there is a

positive correlation between A and B values for all IP types. This positive correlation supports the view that A and B values can be used to estimate CDL for IP types.

Disclosures

Ethics Committee Approval: This study was conducted with the approval taken from the Institutional Clinical Research Ethics Committee University of Health Sciences Istanbul Training and Research Hospital (No: 352, dated 11.11.2022).

Peer-review: Externally peer-reviewed.

Conflict of Interest: None declared.

Authorship Contributions: Concept – D.O.A., Y.K.; Design – D.O.A., E.M.; Supervision – D.O.A., A.S.M., O.M.; Data collection and/or processing – E.M., Y.K.; Analysis and/or interpretation – E.M., Y.K., M.B.U.; Literature review – O.M., A.S.M., M.B.U.; Writing – D.O.A., E.M.; Critical review – D.O.A., E.M., Y.K., M.B.U., O.M., A.S.M.

References

1. Sennaroğlu L, Bajin MD. Classification and current management of inner ear malformations. *Balkan Med J* 2017;34:397-411. [\[CrossRef\]](#)
2. Joshi VM, Navlekar SK, Kishore GR, Reddy KJ, Kumar EC. CT and MR imaging of the inner ear and brain in children with congenital sensorineural hearing loss. *Radiographics* 2012;32:683-98. [\[CrossRef\]](#)
3. Purcell D, Johnson J, Fischbein N, Lalwani AK. Establishment of normative cochlear and vestibular measurements to aid in the diagnosis of inner ear malformations. *Otolaryngol Head Neck Surg* 2003;128:78-87. [\[CrossRef\]](#)
4. Purcell DD, Fischbein N, Lalwani AK. Identification of previously "undetectable" abnormalities of the bony labyrinth with computed tomography measurement. *Laryngoscope* 2003;113:1908-11. [\[CrossRef\]](#)
5. Shim HJ, Shin JE, Chung JW, Lee KS. Inner ear anomalies in cochlear implantees: importance of radiologic measurements in the classification. *Otol Neurotol* 2006;27:831-7. [\[CrossRef\]](#)
6. Chen JL, Gittleman A, Barnes PD, Chang KW. Utility of temporal bone computed tomographic measurements in the evaluation of inner ear malformations. *Arch Otolaryngol Head Neck Surg* 2008;134:50-6. [\[CrossRef\]](#)
7. Lan MY, Shiao JY, Ho CY, Hung HC. Measurements of normal inner ear on computed tomography in children with congenital sensorineural hearing loss. *Eur Arch Otorhinolaryngol* 2009;266:1361-4. [\[CrossRef\]](#)
8. Eser MB, Atalay B, Kalcioğlu MT. Is cochlear length related to congenital sensorineural hearing loss: preliminary data. *J Int Adv Otol* 2021;17:1-8. [\[CrossRef\]](#)
9. Atalay B, Eser MB, Kalcioğlu MT, Ankaralı H. Comprehensive analysis of factors affecting cochlear size: a systematic review and meta-analysis. *Laryngoscope* 2022;132:188-97. [\[CrossRef\]](#)
10. Pamuk G, Pamuk AE, Akgöz A, Bajin MD, Özgen B, Sennaroğlu L. Radiological measurement of cochlear dimensions in cochlear hypoplasia and its effect on cochlear implant selection. *J Laryngol Otol* 2021;135:501-7. [\[CrossRef\]](#)

11. Liu YK, Qi CL, Tang J, Jiang ML, Du L, Li ZH, et al. The diagnostic value of measurement of cochlear length and height in temporal bone CT multiplanar reconstruction of inner ear malformation. *Acta Otolaryngol* 2017;137:119-26. [\[CrossRef\]](#)
12. Escudé B, James C, Deguine O, Cochard N, Eter E, Fraysse B. The size of the cochlea and predictions of insertion depth angles for cochlear implant electrodes. *Audiol Neurootol* 2006;11 Suppl 1:27-33. [\[CrossRef\]](#)
13. Xu J, Xu SA, Cohen LT, Clark GM. Cochlear view: postoperative radiography for cochlear implantation. *Am J Otol* 2000;21:49-56. [\[CrossRef\]](#)
14. Schurzig D, Timm ME, Lexow GJ, Majdani O, Lenarz T, Rau TS. Cochlea helix and duct length identification-evaluation of different curve fitting techniques. *Cochlear Implants Int* 2018;19:268-83. [\[CrossRef\]](#)
15. Sennaroglu L, Saatci I. Unpartitioned versus incompletely partitioned cochleae: radiologic differentiation. *Otol Neurotol* 2004;25:520-9. [\[CrossRef\]](#)
16. Teissier N, Van Den Abbeele T, Sebag G, Elmaleh-Berges M. Computed tomography measurements of the normal and the pathologic cochlea in children. *Pediatr Radiol* 2010;40:275-83. [\[CrossRef\]](#)
17. Dhanasingh A. Variations in the Size and shape of human cochlear malformation types. *Anat Rec (Hoboken)* 2019;302:1792-9. [\[CrossRef\]](#)
18. Meng J, Li S, Zhang F, Li Q, Qin Z. Cochlear size and shape variability and implications in cochlear implantation surgery. *Otol Neurotol* 2016;37:1307-13. [\[CrossRef\]](#)
19. Khurayzi T, Almuhawwas F, Alsanosi A, Abdelsamad Y, Doyle Ú, Dhanasingh A. A novel cochlear measurement that predicts inner-ear malformation. *Sci Rep* 2021;11:7339. [\[CrossRef\]](#)
20. Alexiades G, Dhanasingh A, Jolly C. Method to estimate the complete and two-turn cochlear duct length. *Otol Neurotol* 2014;36:904-7. [\[CrossRef\]](#)
21. Erixon E, Rask-Andersen H. How to predict cochlear length before cochlear implantation surgery. *Acta Otolaryngol* 2013;133:1258-65. [\[CrossRef\]](#)
22. Adunka O, Unkelbach MH, Mack MG, Radeloff A, Gstoettner W. Predicting basal cochlear length for electric-acoustic stimulation. *Arch Otolaryngol Head Neck Surg* 2005;131:488-92. [\[CrossRef\]](#)
23. Avci E, Nauwelaers T, Lenarz T, Hamacher V, Kral A. Variations in microanatomy of the human cochlea. *J Comp Neurol* 2014;522:3245-61. [\[CrossRef\]](#)